AMERICAN SOCIETY FOR MICROBIOLOGY | Journal of Virology®

VIRUS-CELL INTERACTIONS

Reduced Potency and Incomplete Neutralization of Broadly Neutralizing Antibodies against Cell-to-Cell Transmission of HIV-1 with Transmitted Founder Envs

Hongru Li,[a,b] Chati Zony,[a,b] Ping Chen,[b] Benjamin K. Chen[a,b]

Microbiology Graduate School Training Program, Department of Microbiology,[a] and Division of Infectious Disease, Department of Medicine, Immunology Institute,[b] Icahn School of Medicine at Mount Sinai, New York, New York, USA

ABSTRACT Broadly neutralizing antibodies (bNAbs) have been isolated from HIV-1 patients and can potently block infection of a wide spectrum of HIV-1 subtypes. These antibodies define common epitopes shared by many viral isolates. While bNAbs potently antagonize infection with cell-free virus, inhibition of HIV-1 transmission from infected to uninfected $CD4^+$ T cells through virological synapses (VS) has been found to require greater amounts of antibody. In this study, we examined two well-studied molecular clones and two transmitted/founder (T/F) clones for their sensitivities to a panel of bNAbs in cell-free and cell-to-cell infection assays. We observed resistance of cell-to-cell transmission to antibody neutralization that was reflected not only by reductions of antibody potency but also by decreases in maximum neutralization capacity relative to the levels seen with cell-free infections. BNAbs targeting different epitopes exhibited incomplete neutralization against cell-associated virus with T/F Envs, which was not observed with the cell-free form of the same virus. We further identified the membrane-proximal internal tyrosine-based sorting motif as a determinant that can affect the incomplete neutralization of these T/F clones in cell-to-cell infection. These findings indicate that the signal that affects surface expression and/or internalization of Env from the plasma membrane can modulate the presentation of neutralizing epitopes on infected cells. These results highlight that a fraction of virus can escape from high concentrations of antibody through cell-to-cell infection while remaining sensitive to neutralization in cell-free infection. The ability to fully inhibit cell-to-cell transmission may represent an important consideration in the development of antibodies for treatment or prophylaxis.

IMPORTANCE In recent years, isolation of new-generation HIV-1 bNAbs has invigorated HIV vaccine research. These bNAbs display remarkable potency and breadth of coverage against cell-free virus; however, they exhibit a diminished ability to block HIV-1 cell-to-cell transmission. The mechanism(s) by which HIV-1 resists neutralization when transmitting through VS remains uncertain. We examined a panel of bNAbs for their ability to neutralize HIV-1 T/F viruses in cell-to-cell infection assays. We found that some antibodies exhibit not only reduced potency but also decreased maximum neutralization capacity or *in vitro* efficacy against cell-to-cell infection of HIV-1 with T/F Envs compared to cell-free infection of the same virus. We further identified the membrane-proximal internal tyrosine-based sorting motif YXXL as a determinant that can affect the incomplete neutralization phenotype of these T/F clones. When the maximum neutralization capacity falls short of 100%, this can have a major impact on the ability of antibodies to halt viral replication.

KEYWORDS human immunodeficiency virus subtype 1 (HIV-1), HIV-1 envelope (Env),

Received 19 December 2016 **Accepted** 18 January 2017

Accepted manuscript posted online 1 February 2017

Citation Li H, Zony C, Chen P, Chen BK. 2017. Reduced potency and incomplete neutralization of broadly neutralizing antibodies against cell-to-cell transmission of HIV-1 with transmitted founder Envs. J Virol 91:e02425-16. https://doi.org/10.1128/JVI.02425-16.

Editor Guido Silvestri, Emory University

Address correspondence to Benjamin K. Chen, ben.chen@mssm.edu.

For a commentary on this article, see https://doi.org/10.1128/JVI.00149-17.

cell-to-cell infection, virological synapse (VS), broadly neutralizing antibodies (bNAbs), efficacy, potency, maximum neutralization, incomplete neutralization, tyrosine-based sorting motif

Infections by HIV-1 can be initiated by both cell-free and cell-associated virus. Cell-free infection occurs when virus particles are released from infected cells and infect HIV-1 naive target $CD4^+$ T cells at a distance. Cell-to-cell infection is mediated by adhesive cell-cell contacts that form between infected and uninfected $CD4^+$ T cells (called "virological synapses" [VS]). Cell-to-cell infection through VS is more efficient than cell-free infection *in vitro* (1, 2) and has been found to resist neutralizing antibodies (NAbs) to a greater extent than infection by the same viral clone when it is presented as cell-free virus (1, 3–11).

A VS between infected and uninfected T cells was initially described as an actin-dependent recruitment of viral proteins Gag and Env on the infected cell and CD4 on uninfected target T cell to the site of cell-cell contact (12). The formation of VS is dependent on interaction between Env and CD4 (1, 12, 13). Different models that have been proposed for T cell VS-mediated transmission are distinguished by the extent to which cell-free virions accumulate at the cell-cell interface. While it has been suggested that cell-free particles may gather at the cell-cell junction and fuse at the cell surface (8, 12, 14), other studies indicate that HIV-1 is first transferred across VS in a coreceptor-independent manner (1, 14–18) and is concentrated in trypsin-resistant endocytic compartments where viral fusion occurs (1, 18). In live imaging studies of VS formation, Env/CD4-dependent cell adhesion can be observed before Gag is recruited to the site of cell-cell contact, indicating that Env may first function as a cell adhesion molecule even prior to the time at which the virus particle is formed (16). After transfer of HIV-1 into trypsin-resistant endocytic compartments within target cells, maturation of virus particles and fusion of single particles within the target cell have also been observed (18). However, it remains unclear to what extent viral entry from the plasma membrane or from internal endosomal sites may occur.

HIV-1 patients make abundant antibodies against Env during the course of chronic infection. In recent years, many broadly neutralizing antibodies (bNAbs) with remarkable breadth and potency have been isolated from chronically infected HIV-1 patients (19–32). Many of these bNAbs have been shown to be capable of inhibiting up to 90% of circulating viral strains in *in vitro* studies. When these antibodies are passively transferred, they can provide protective immunity against challenges with chimeric simian-human immunodeficiency viruses (SHIVs) in macaques and against HIV-1 in humanized mice (33–37). When administered in combination, bNAbs cocktails can dramatically reduce viremia in infected animals (38–41).

Existing bNAbs were initially characterized based on their ability to neutralize a broad range of cell-free primary isolate Env-pseudotyped viruses in TZM-bl reporter cell assays (42). Potencies of bNAbs defined by 50% inhibitory concentration (IC_{50}) or IC_{80} values in such assays have been the main criteria for clinical candidates. However, several new-generation bNAbs with remarkable potency and breadth have been found to block cell-to-cell infection considerably less effectively than cell-free infection and this is even clearer in examining HIV-1 primary isolates (3–7, 9, 10). The magnitude of resistance is dependent on both the targeted epitopes and the viral strains (7). The mechanisms that promote resistance of cell-associated HIV-1 to neutralization by bNAbs are still unclear. It has been reported that truncation of the Env cytoplasmic tail (CT) enhanced neutralization sensitivity in cell-to-cell infection whereas the same mutation had a very modest impact on cell-free infection (3). Given that the CT plays an important role in inhibiting fusion of immature virus particles (43–46), it has been proposed that the neutralization resistance of cell-associated HIV-1 is related to the regulation of Env conformational states (3). Truncation of the Env CT can change the binding of bNAbs and nonneutralizing antibodies to Env on transfected cells (47), indicating that Env can assume different conformational states that may be differen-

tially regulated by CT through inside-out signaling. Truncation of the Env CT to different extents can also alter the capacity of Env to infect through cell-free or cell-to-cell routes (48).

Besides potency, another important pharmacological parameter to consider in analysis of the therapeutic effects of bNAbs *in vivo* is "efficacy," defined as the maximum response achievable in a dose-effect relationship in therapeutics (49). The Burton group recently reported reduced efficacy of several bNAbs in cell-free neutralization assays and described the results as representative of "incomplete neutralization" (50). This finding underscored the importance of characterizing the efficacy of bNAbs for their clinical use and for vaccine designs, as the use of a resistant viral population would result in failed viral control in patients. Differences in the fractions of incomplete neutralization of HIV-1 in comparisons of cell-to-cell infection with cell-free infection have not been reported.

Here we tested two well-studied HIV-1 Envs and a pair of HIV-1 transmitted/founder (T/F) Envs for their cell-free and cell-to-cell neutralization sensitivities to a panel of bNAbs. We observed that the level of resistance of cell-to-cell HIV-1 transmission to antibody neutralization relative to that of cell-free infection was reflected not only in reductions in antibody potency but also in major decreases in maximum neutralization capacity, or maximum *in vitro* efficacy. The ability of a tyrosine-based sorting signal within Env to modulate this maximum neutralizing capacity phenotype underscores the concept that HIV-1 cell-to-cell transmission may be influenced by signals that regulate the recycling of Env from the plasma membrane.

RESULTS

Resistance of transmitted founder (T/F) virus Envs to pooled HIV-1-positive patient IgG (HIVIG) during VS cell-to-cell transmission. Two subtype B T/F HIV-1 Envs (QH0692 and RHPA) as well as laboratory-adapted NL4-3 Env and a chronic R5-tropic JR-FL Env were cloned in the context of a fluorescent protein-expressing HIV-1 construct (NL4-3 Cherry internal ribosome entry site [NLCI]; Fig. 1A). These viral constructs allowed us to examine the ability of neutralizing antibodies to inhibit cell-free and cell-associated HIV-1 infection of T/F viruses and to compare T/F Env genes with NL4-3 Env or JR-FL genes where the only differences between the clones were in the Env glycoprotein. We chose these two T/F Env clones from a panel of clade B isolates because they exhibited intermediate sensitivity to neutralization, they have been defined as tier 2 isolates (42), and their infectivity is readily measured in the context of HIV-1 clone NL4-3 (data not shown). The T/F Env-expressing clones produced virus particles in transfected 293T cells at levels similar to those seen with clones expressing laboratory-adapted NL4-3 Env or chronic R5-tropic virus JR-FL Env (Fig. 1B and C). The single-round cell-free and cell-to-cell infection assays utilized here were performed using flow cytometry. To measure the contribution of cell-free infection from virus produced by infected donor cells during the course of cell-cell coculture, we performed a transwell assay (Fig. 1D) where donor and target cells were separated by a virus-permeable barrier. This assay was performed side by side with a single-round cell-to-cell infection assay. With comparable levels of cell-associated viral input, the percentage of infection from free virus produced from nucleofected Jurkat cells was 0.49%, while the level of infection from direct cell-cell coculture was found to be 17.1% (Fig. 1D). Therefore, the cell-to-cell infection assay allowed us to measure cell-to-cell infection with only minor contributions from cell-free virus (Fig. 1D). Furthermore, we note that because the background infection signal was very low, the assay can also detect low-level infections with high sensitivity (Fig. 1E and F).

We first tested the viruses for their neutralization by pooled HIV-1 immune gamma globulin (HIVIG; Luiz Barbosa, AIDS Reagent Program [ARP]). At the highest concentration, HIVIG blocked cell-free infection in laboratory-adapted strain $NLCI_{NL4-3}$ and R5-tropic chronic clone $NLCI_{JR-FL}$ as well as $NLCI_{QH0692}$ and $NLCI_{RHPA}$ (Fig. 2A). In contrast, in cell-to-cell neutralization assays, HIVIG inhibited only laboratory isolate $NLCI_{NL4-3}$ and chronic clone $NLCI_{JR-FL}$ and not the two T/F Env clones. $NLCI_{QH0692}$, $NLCI_{RHPA}$, and

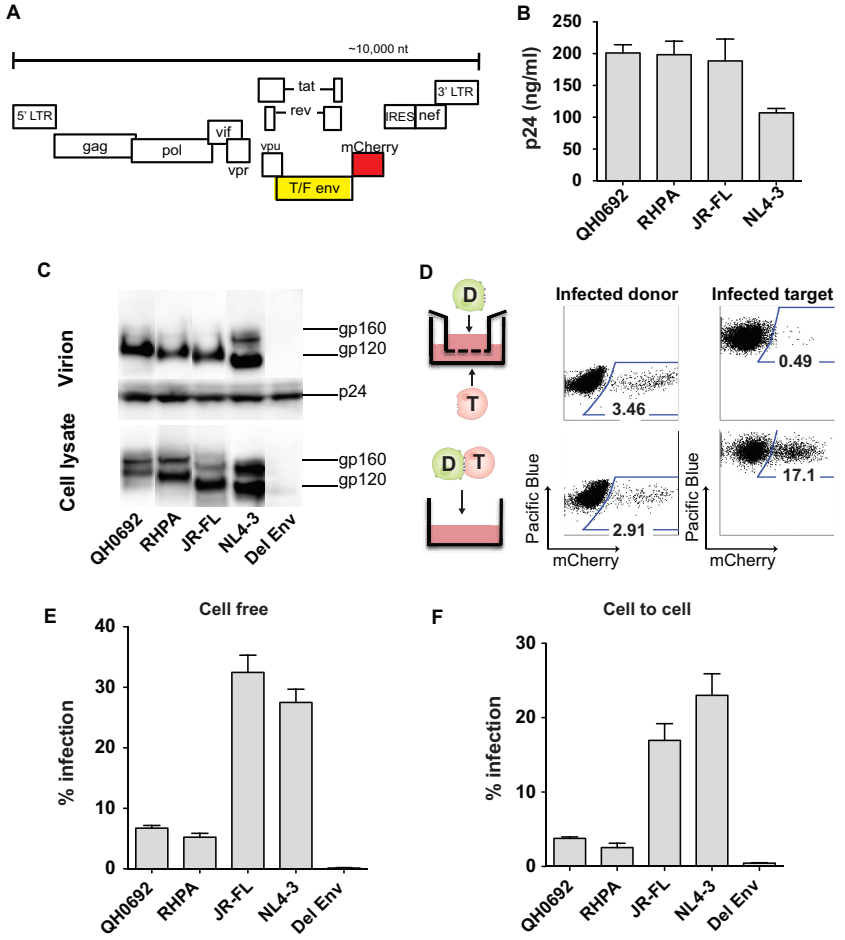

FIG 1 Characterization of fluorescent protein-expressing proviral molecular clone of HIV-1 with T/F Env. (A) Cloning scheme of introducing T/F Env into fluorescent protein-expressing proviral molecular clone NLCI. LTR, long terminal repeat. (B) Viral production in transfected 293T cells was measured by p24 ELISA. Mean values from three independent experiments are shown. Error bars represent standard errors of the means. (C) Env expression in transfected 293T cells and Env incorporation into viral particles were examined by Western blotting. The amount of sample loaded was normalized to the sample p24 content. (D) Representative flow cytometry plots of transwell assay and cell-to-cell coculture system for comparison side by side. For the transwell assay, nucleofected Jurkat donor cells and MT4R5 target cells were separated into two compartments by a membrane with a pore size of 0.4 μm, which allows passage of cell-free virus particles. A cell-to-cell coculture infection was performed at the same time under similar conditions. To inhibit secondary rounds of infection, AZT (10 μM) was added 18 h postinfection. (E) Single-round cell-free infection in CD4$^+$ CCR5-expressing MT4R5 cells. Cell-free infection was normalized to the p24 input. Del, deleted. (F) Single-round cell-to-cell infection levels of MT4R5 target cells from coculture of Jurkat donor cells transfected with NLCI constructs with T/F Env. Cell-to-cell infection was normalized to same percentage of donor transfection and the donor target ratio. Error bars represent results of three independent experiments.

$NLCI_{NL4-3}$ were also tested for cell-free and cell-to-cell neutralization sensitivity to individual patient IgG isolated from three HIV-1 patients (Fig. 2B). Patient-specific differences in IgG responses and in their abilities to neutralize different viral isolates were observed (Fig. 2B and data not shown). Viruses with T/F Envs were 2-fold to 24-fold more resistant to neutralization by patient IgG than laboratory-adapted strain $NLCI_{NL4-3}$ in cell-free infection and 1.5-fold to 4-fold more resistant in cell-to-cell infection in comparisons of IC_{50} values (Table 1). For the virus/IgG combinations tested, cell-free infection could be neutralized at up to 80% (except for patient 3 IgG with $NLCI_{RHPA}$), and cell-to-cell infection consistently displayed greater resistance to neutralization than cell-free infection.

Resistance of T/F virus Envs to bNAbs during cell-to-cell transmission. Next, we investigated whether certain epitopes of HIV-1 Env are preferentially involved in the

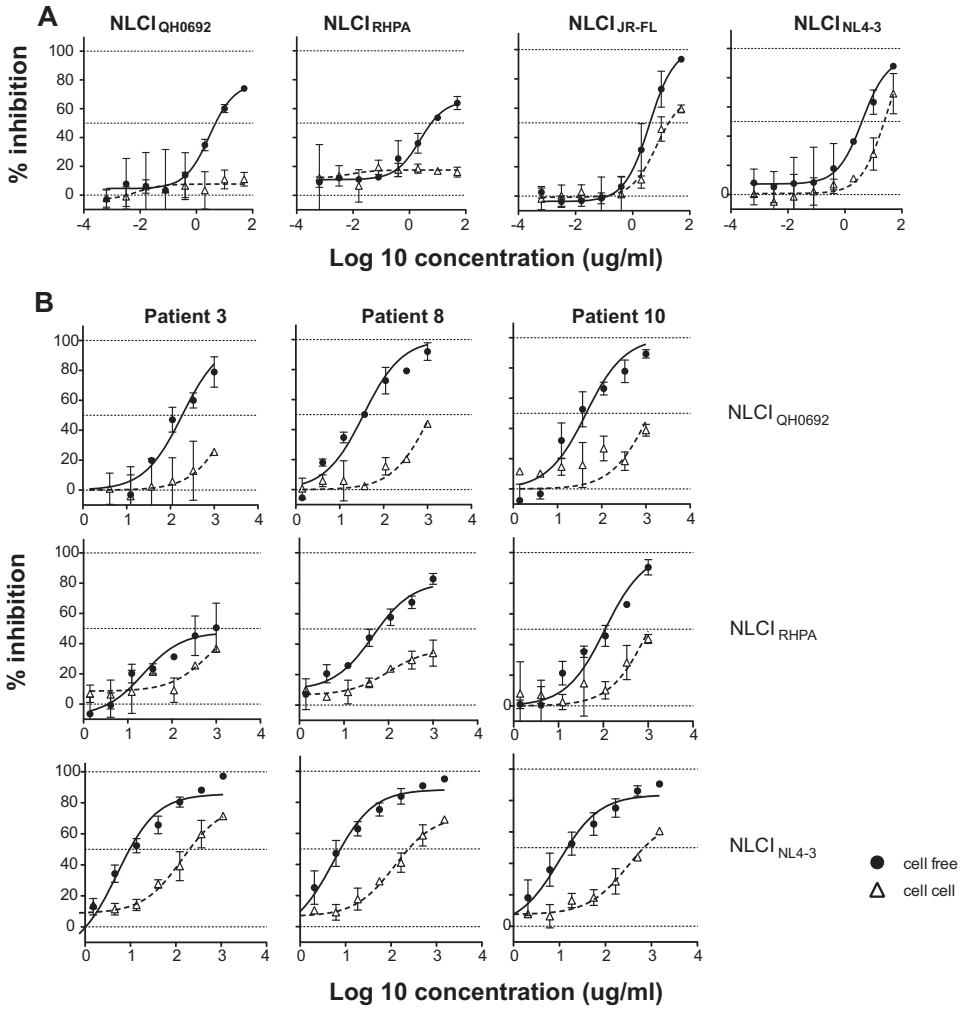

FIG 2 Relative levels of resistance to neutralizing HIV-1 patient IgG (HIVIG) in HIV-1 cell-to-cell transmission. (A) Single-round neutralization experiments using the two HIV-1 T/F Envs, laboratory-adapted NL4-3 Env, and chronic R5-tropic JR-FL Env NLCI constructs with pooled HIV-1-positive patient IgG (HIVIG) in cell-free infection (closed circle with solid lines) and cell-to-cell infection (open triangles with dotted lines). HIVIG was serially 3-fold diluted starting from 50 μg/ml. (B) $NLCI_{QH0692}$ (top), $NLCI_{RHPA}$ (middle), and $NLCI_{NL4-3}$ (bottom) were tested for cell-free and cell-to-cell neutralization sensitivity to single-patient IgG isolated from plasma from three chronically infected HIV-1 patients. Single-patient IgG was purified by the use of protein AG beads and serially diluted 1:3 starting from 1 mg/ml.

differential resistance of cell-to-cell transmission over cell-free infection. We used the following panel of bNAbs targeting major defined sites of vulnerability on HIV-1 Env: (i) glycan patch-recognizing antibody 2G12; (ii) CD4bs antibodies VRC01 and HJ16; (iii) membrane-proximal external region (MPER) antibodies 2F5 and 4E10; (iv) gp120/gp41 interface antibody 35O22; (v) V1/V2 apex antibody PG9; and (vi) glycan-dependent V3 antibodies PGT121, PGT126, and 10-1074.

As a control, we tested the anti-CD4 monoclonal antibody (MAb) Leu3a (BD Biosciences). It was found to abrogate HIV-1 infection through both the cell-free and cell-to-cell routes with similar efficiency (Fig. 3A). Glycan patch-binding MAb 2G12 blocked cell-free infection in strains $NLCI_{QH0692}$, $NLCI_{JR-FL}$, and $NLCI_{NL4-3}$ but not strain $NLCI_{RHPA}$ (Fig. 3B).

CD4bs MAb VRC01 potently neutralized cell-free infection of all four viruses, and HJ16 could inhibit all but $NLCI_{JR-FL}$ (Fig. 3C). QH0692 and RHPA Envs are categorized as tier 2 with respect to their cell-free neutralization sensitivity using a standard TZM-bl assay, and both the QH0692 Envs and the RHPA Envs exhibited a higher IC_{50} for VRC01 than laboratory strain $NLCI_{NL4-3}$ and chronic clone $NLCI_{JR-FL}$ (Fig. 3C, top). For all four

TABLE 1 IC_{50} of cell-free neutralization with HIVIG and single-patient IgG

Strain	Ig source[a]	IC_{50} under indicated transmission conditions	
		Cell free	Cell to cell
$NLCI_{QH0692}$	HIVIG	4.7	>50
	Pt 3	186	>1,000
	Pt 8	35	>1,000
	Pt 10	44.6	>1,000
$NLCI_{RHPA}$	HIVIG	6	>50
	Pt 3	>1,000	>1,000
	Pt 8	58.2	>1,000
	Pt 10	110	>1,000
$NLCI_{NL4-3}$	HIVIG	4	24
	Pt 3	13.1	271
	Pt 8	7.7	242
	Pt 10	14.8	684
$NLCI_{JR-FL}$	HIVIG	4	18.2

[a]Pt, patient.

virus strains, cell-to-cell infection was generally more resistant to VRC01. The fold change of IC_{50} in cell-to-cell infection over cell-free infection ranged from 3.7 to 45.7 (Fig. 3). HJ16 (Fig. 3C, bottom) showed higher potency (lower IC_{50}) against $NLCI_{QH0692}$ and $NLCI_{RHPA}$ in cell-free neutralization; however, even higher concentrations of antibody were required to block cell-to-cell infection for both $NLCI_{QH0692}$ and $NLCI_{RHPA}$. Notably, at a saturating concentration of HJ16, more than 95% of $NLCI_{RHPA}$ cell-free infection was blocked whereas only 60% of cell-to-cell infection was inhibited. This indicates that there was a large fraction of the cell-associated virus that was completely resistant to HJ16.

MPER MAb 2F5 neutralized the four viruses by greater than 95% in cell-free neutralization assays (Fig. 3D), while in cell-to-cell neutralization, a 48-fold to 368-fold-higher concentration of antibody was required to achieve 50% inhibition than in the cell-free route. Notably, for $NLCI_{RHPA}$, the maximum neutralization capacity of 2F5 was slightly higher than 50% of the total infection, indicating that only about 50% of the cell-associated virus was sensitive to the antibody. Another MPER antibody, 4E10 (Fig. 3D), was less potent than 2F5 against cell-free virus and showed similarly decreased potency and maximum efficacy against cell-associated HIV. The fold difference of IC_{50} in cell-to-cell infection over infection with cell-free virus was dependent upon the viral strain tested. A greater IC_{50} shift was seen in $NLCI_{QH0692}$ than in the other three viruses.

A gp120/gp41 interface antibody, 35O22, displayed the largest IC_{50} difference in cell-to-cell neutralization over cell-free neutralization (Fig. 3E). It exhibited an IC_{50} to block cell-to-cell infection that was a remarkable 3,400-fold higher than that seen with cell-free infection with $NLCI_{QH0692}$ and about 7-fold higher than that seen with $NLCI_{NL4-3}$.

The V1/V2 apex-targeting MAb PG9 was not potent in either cell-free or cell-to-cell neutralization with the viruses tested (Fig. 3F). It inhibited cell-free infection and cell-to-cell infection using $NLCI_{RHPA}$ and $NLCI_{NL4-3}$ with low potency. Glycan-dependent V3 antibodies PGT121, PGT126, and 10-1074 inhibited cell-free infection potently, except with $NLCI_{NL4-3}$. The cell-associated infection again required greater amounts of antibody to block, and there was a range of fold change in IC_{50} from 0.8 to more than 2,400 seen in comparisons of cell-free and cell-associated infections (Fig. 3G). Interestingly, we note that in all the combinations of T/F constructs assayed with this panel of V3 antibodies, cell-free infection could be almost completely inhibited, with the exception of the combination of PGT121 and $NLCI_{QH0692}$, while maximal levels of inhibition of cell-to-cell infection were all below 80%. These antibodies therefore showed a large fraction of noninhibited infection, which is indicative of incomplete neutralization.

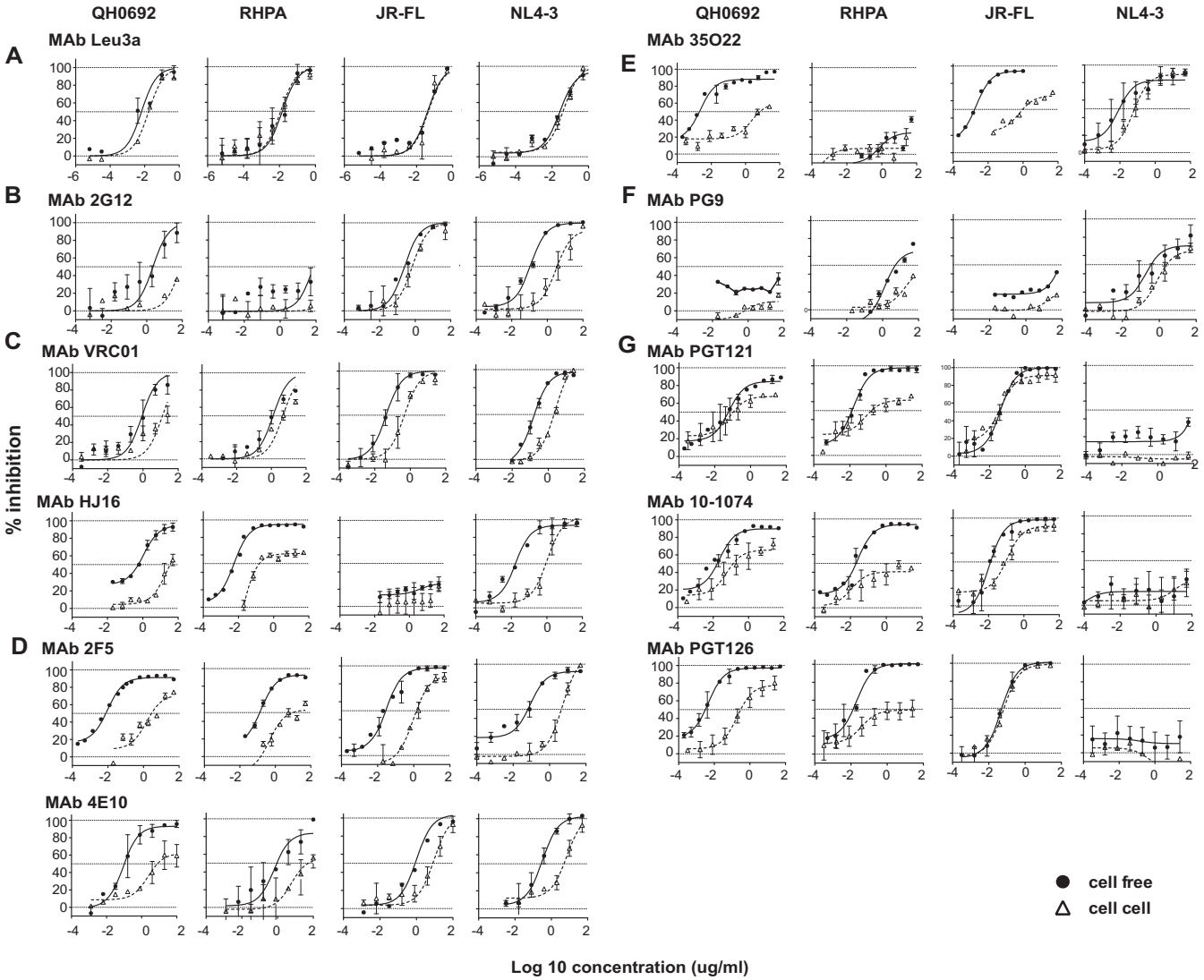

FIG 3 Relative levels of resistance to broadly neutralizing MAbs in HIV-1 cell-to-cell transmission. Single-round cell-free and cell-to-cell neutralization assays were performed using NLCI constructs with T/F Env clones QH0692 and RHPA, laboratory-adapted NL4-3 Env, and chronic R5-tropic JR-FL Env. Error bars represent mean values and standard errors of the means (SEM) of results from duplicates of at least two independent experiments conducted on different dates. Antibodies targeting different sites of vulnerability on HIV-1 Env were tested. (A) CD4 blocking antibody Leu3a. (B) MAb targeting glycan epitope 2G12. (C) MAb targeting CD4bs VRC01 and HJ16. (D) MAb targeting membrane-proximal external region 2F5 and 4E10. (E) MAb targeting gp120/gp41 interface 35O22. (F) MAb targeting glycan-dependent V1/V2 epitope PG9. (G) MAb targeting V3 glycans PGT121, PGT126, and 10-1074. Each antibody was studied for its neutralization activity against cell-free infection and cell-to-cell infection. Cell-free neutralization curves are shown with closed circles and solid lines, and cell-to-cell neutralization curves are shown with open triangles and dotted lines.

IC_{50}s and maximum neutralization percentages of all bNAbs in cell-free and cell-to-cell infection assays of the four viruses are listed in Table 2.

Relative levels of resistance of HIV-1 cell-to-cell transmission are reflected in the reduction of potency and maximum efficacy of bNAbs. As shown above, for nearly all bNAbs tested, cell-to-cell infection was generally more resistant to antibody neutralization than cell-free infection, except for Leu3a, which binds to the gp120-binding site on CD4. The fold increase of IC_{50} in cell-to-cell neutralization compared to the cell-free route is displayed in a heat map representation (Fig. 4A). Almost all bNAbs (with the exception of CD4 blocking antibody leu3a) blocked cell-free infection with higher potency, as reflected by fold increases in IC_{50} of >1.

Infection with cell-free virus could be inhibited by more than 95% in most cases (Fig. 3), whereas the percentage of maximum inhibition at saturating concentrations of antibody in cell-to-cell infections was as low as 36% (Fig. 3C, D, E, and G). We plotted

TABLE 2 IC_{50} and percent maximum neutralization with bNAbs

Strain	bNAb	Value under indicated transmission conditions			
		Cell free		Cell to cell	
		IC_{50}	% maximum neutralization	IC_{50}	% maximum neutralization
$NLCI_{QH0692}$	Leu3a	0.01	100	0.02	100
	2G12	2.24	90.5	83.0	35.9[a]
	VRC01	0.28	93.2	12.6	51.5[a]
	HJ16	0.56	92.8	34.8	55.3[a]
	2F5	0.008	91.8	2.8	74.3
	4E10	0.1	95.8	7.4	59.2
	35O22	0.002	97.2	6.9	56.1
	PG9	NA[b]	NA	NA	NA
	PGT121	0.058	89.1	0.1	69.7
	10-1074	0.02	91.1	0.14	74
	PGT126	0.003	98.9	0.3	80
$NLCI_{RHPA}$	Leu3a	0.01	100	0.01	100
	2G12	NA	NA	NA	NA
	VRC01	1.3	80[a]	4.6	66.7[a]
	HJ16	0.004	96.6	0.17	62.1
	2F5	0.13	90.1	9.5	60.4
	4E10	1.3	99.2	146	55.8[a]
	35O22	NA	NA	NA	NA
	PG9	5.1	73.5[a]	>50	38.2[a]
	PGT121	0.013	96.0	0.16	66.1
	10-1074	0.021	90.3	>25	44.8
	PGT126	0.013	100	>25	42.1
$NLCI_{NL4-3}$	Leu3a	0.03	96.5	0.04	96.4
	2G12	0.1	99.9	3.6	95.5
	VRC01	0.17	96.9	2.1	98.9
	HJ16	0.02	96.6	0.9	97.2
	2F5	0.06	93.1	4.5	99
	4E10	0.3	99.4	5.9	94.5
	35O22	0.01	90.1	0.07	92.9
	PG9	0.36	81.9[a]	2.5	72[a]
	PGT121	NA	NA	NA	NA
	10-1074	NA	NA	NA	NA
	PGT126	NA	NA	NA	NA
$NLCI_{JR-FL}$	Leu3a	0.04	97.7	0.1	94.7
	2G12	0.3	97.8	0.7	90.9
	VRC01	0.04	96.0	0.5	94.7
	HJ16	NA	NA	NA	NA
	2F5	0.03	99.8	1.4	90.1
	4E10	1.0	96.1	9.2	95.6
	35O22	0.002	96.4	1.0	70.1[a]
	PG9	NA	NA	NA	NA
	PGT121	0.04	99.8	0.03	97.5
	10-1074	0.01	100	0.09	97.4
	PGT126	0.1	100	0.07	100

[a]The maximum percentage of inhibition detected in these assays was not saturated at the highest concentration tested.
[b]NA, not active, due to low inhibitory activity.

maximal percent inhibition of cell-free infection and cell-to-cell infection and found that MAb at saturating concentrations inhibited cell-to-cell infection with significantly lower maximal percent inhibition than infection with cell-free virus (Fig. 4B, top). For the antibody panel tested, this incomplete neutralization phenotype was evident with two T/F Envs, QH0692 and RHPA, and was not apparent with the laboratory-adapted NL4-3 Env or the chronic R5-tropic JR-FL Env (Fig. 4B, bottom).

Impact of producer cell and glycosylation on potency and efficacy of bNAbs. To investigate if the incomplete neutralization observed in cell-to-cell infection could be attributed mainly to cell-specific properties associated with the viral producer cells, we

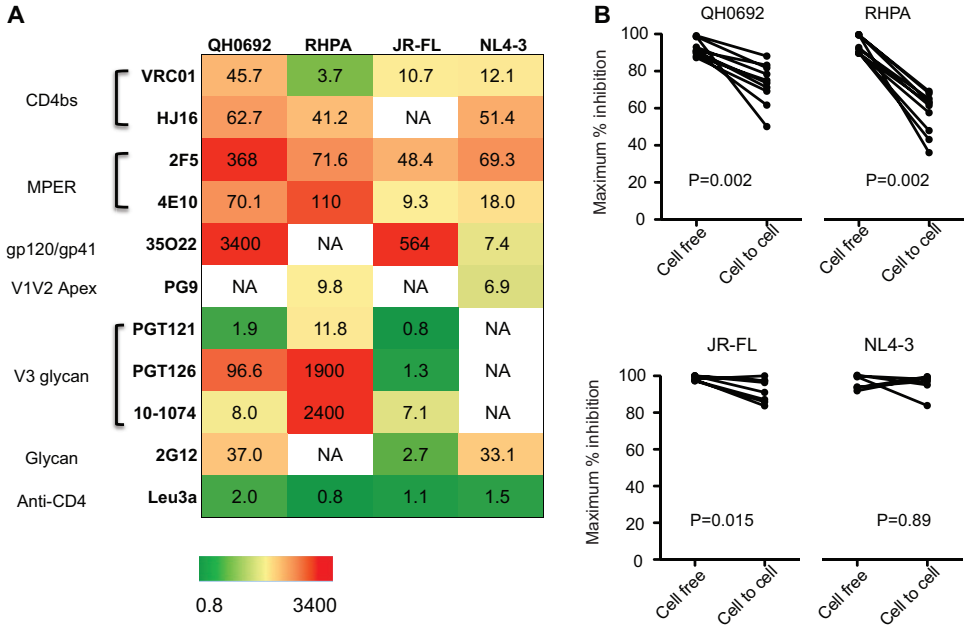

FIG 4 Relative levels of resistance of HIV-1 cell-to-cell infection to neutralization is reflected in diminished potency and efficacy of bNAbs. (A) The table indicates the degree to which cell-to-cell infection is less efficiently neutralized than cell-free infection, indicating the fold increase in the 50% inhibitory concentration for each antibody-virus combination tested. Numbers represent mean values of results from duplicates of at least two independent experiments. (B) Maximum efficacy represented by the maximal percentages of inhibition at saturating concentrations of MAbs in cell-to-cell infection and cell-free infection were plotted and compared using a Wilcoxon matched-pair test. *P* values for the Wilcoxon analysis are indicated for T/F Envs (top) and laboratory-adapted NL4-3 or chronic JR-FL Env (bottom).

generated cell-free virus from the Jurkat T cell line, which is the same cell type as the donor cells used in the cell-to-cell infection assays. When 293T-produced and Jurkat-produced cell-free viruses were tested side by side for neutralization sensitivity to glycan-dependent V3 MAbs, Jurkat cell-produced cell-free virus could be completely neutralized (Fig. 5A). The cell-free neutralization curves seen with Jurkat-produced cell-free $NLCI_{RHPA}$ virus were nearly identical to the curves observed with virus produced in 293T cells in most cases (Fig. 5A). The maximum level of neutralization of Jurkat-produced virus was generally similar to that achieved with 293T-produced virus. Testing $NLCI_{QH0692}$ viruses, however, we observed a large difference in IC_{50}s in comparing virus produced in 293T cells to those from Jurkat cells for the glycan-dependent V3 antibody, 10-1074, but not for PGT121 or PGT126 (Fig. 5A). In the case of 10-1074 MAb, the IC_{50} against cell-free virus produced in Jurkat cells was much higher than that produced in 293 T cells, revealing cell type-specific shifts in neutralization potency.

Virus produced in different cell types can generate virus with heterogeneous glycosylation that can cause cell type-dependent shifts in IC_{50} (51). To investigate if the IC_{50} shift and the changes in maximum neutralization could be attributed to glycosylation heterogeneity, we generated cell-free and cell-associated viral inoculums in the presence and absence of the alpha mannosidase inhibitor kifunensine (Kif; 25 μM) and compared the levels of neutralization sensitivity that resulted from the two routes of viral infection.

Tested against V3 glycan MAbs PGT121, PGT126, and 10-1074, cell-free $NLCI_{QH0692}$ and $NLCI_{RHPA}$ virus produced from transfected 293T cells in the presence of Kif were in most cases more sensitive to antibody neutralization than virus produced in the absence of Kif (Fig. 5B). Large differences in maximum neutralization percentages between Kif-treated and untreated virus were not observed (Fig. 5B). For cell-to-cell infection, nucleofected donor Jurkat cells were also prepared in the presence or absence 25 μM Kif and compared side by side for their susceptibility to the same panel of MAbs. Incomplete (lower than 80%) neutralization was observed with and without

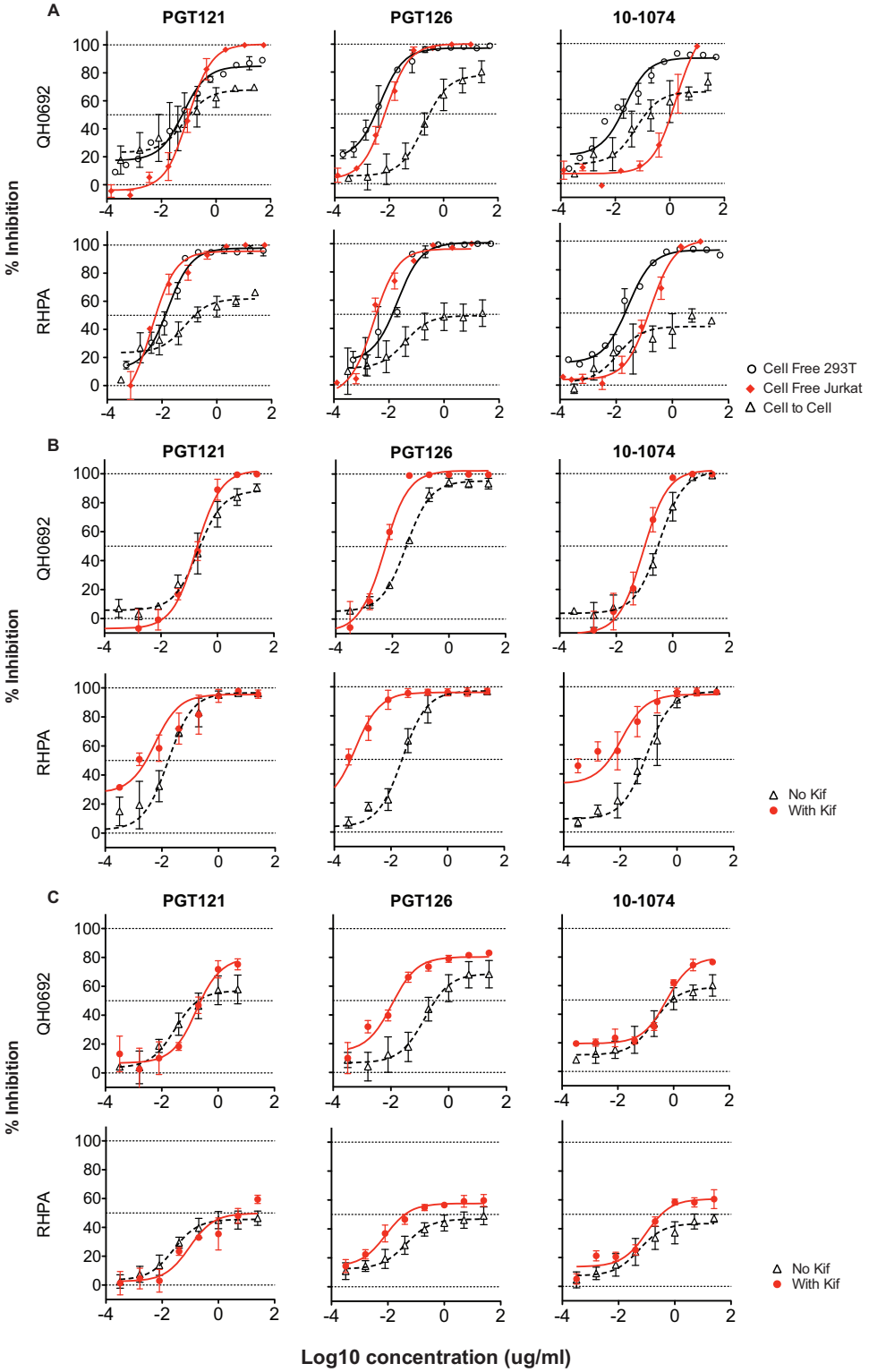

FIG 5 Effect of producer cell or glycosylation on antibody neutralization potency and maximum neutralization capacity. (A) Jurkat-produced cell-free virus was compared with 293T-produced cell-free virus to assess the producer cell type dependence of neutralization by V3 bNAbs PGT121, PGT126, and 10-1074. (B) Cell-free virus produced in the presence and absence of kifunensine was tested for neutralization by the use of V3 glycan MAbs. (C) Cell-associated viral inocula produced in the presence and absence of kifunensine were compared for neutralization sensitivity to V3 glycan MAbs in cell-to-cell infection from Jurkat cells to MT4R5 cells.

Kif. However, we did observe minor increases in the maximum percentages of inhibition in some of the antibody-virus combinations (Fig. 5C). These results indicate that maximum neutralization of bNAbs was not solely due to differences specific to viral producer cells and was not greatly affected by the presence of the kifunensine glycosylation inhibitor.

Mutation in the YXXL endocytosis motif enhanced cell-to-cell neutralization sensitivity. We next hypothesized that the incomplete neutralization phenotypes might be indicative of heterogeneous states of Env that exist on the surface of infected cells. This could be related to dynamic Env trafficking to and from the plasma membrane during cell-cell interactions. Mutants with a disrupted YXXL endocytosis motif within the cytoplasmic tail of gp41, $NLCI_{QH0692\text{-}Y724A}$, and $NLCI_{RHPA\text{-}Y710A}$ were generated (52–54). We first assessed the Env incorporation and processing efficiency of YXXL mutant viral particles by Western blotting and compared the results to those obtained with virus expressing wild-type (WT) Env. Envs with tyrosine mutations were efficiently incorporated into viral particles and processed into gp120 in the QH0692 clone, while the processing efficiency was slightly lower with the RHPA clone (Fig. 6A). $NLCI_{QH0692\text{-}Y724A}$ and $NLCI_{RHPA\text{-}Y710A}$ expressed higher levels of Env on the surface of nucleofected Jurkat T cells than their nonmutated counterparts under conditions of staining with a panel of MAbs, including 2G12, b12, 10-1074, and 2F5 (Fig. 6B). About 1.5-fold more Env binding was observed with glycan-reactive antibody 2G12 (which may be less conformationally dependent) in $NLCI_{QH0692\text{-}Y724A}$ than in wild-type $NLCI_{QH0692}$. Interestingly, the level of surface Env binding seen with $NLCI_{QH0692\text{-}Y724A}$ was about 9-fold higher than the level seen with $NLCI_{QH0692}$ under conditions of staining with b12, 4.5-fold higher than the level seen with 10-1074, and 7.6-fold higher than the level seen with 2F5 (Fig. 6C). Similar results were also observed with $NLCI_{RHPA\text{-}Y710A}$ compared with $NLCI_{RHPA}$ (Fig. 6C), except we noted that 2G12 does not bind RHPA Env.

YXXL mutants $NLCI_{QH0692\text{-}Y724A}$ and $NLCI_{RHPA\text{-}Y710A}$ were then tested for their cell-to-cell neutralization sensitivity with V3-glycan MAbs PGT126 and 10-1074, CD4bs MAb b12, and gp120/gp41 interface MAb 35O22. With the V3 glycan MAbs PGT126 and 10-1074, in contrast to the low (as low as 36%) maximum neutralization that we had previously observed with $NLCI_{QH0692}$ and $NLCI_{RHPA}$, cell-to-cell infection of YXXL mutants could be inhibited by as much as 90%. A slightly lower IC_{50} was observed in $NLCI_{RHPA\text{-}Y710A}$ than in $NLCI_{RHPA}$, while no obvious shift was observed against $NLCI_{QH0692\text{-}Y724A}$ compared with $NLCI_{QH0692}$ (Fig. 6D). With CD4bs MAb b12, dramatic increases in both potency and maximum neutralization were observed in YXXL mutant viruses over WT viruses in cell-to-cell infection (Fig. 6D). Interestingly, in testing with gp120/gp41 interface MAb 35O22, YXXL mutation rendered $NLCI_{QH0692}$ more resistant to antibody neutralization in both cell-free and cell-to-cell infections (Fig. 6D and E). We noted that the $NLCI_{QH0692}$ YXXL mutant exhibited either increased or decreased neutralization sensitivity, depending upon the epitope targeted, indicating that the changes in the neutralization sensitivity of the mutant were not a consequence of increased Env expression levels in infected cells. We suggest that YXXL mutation may affect the conformational states of Env and its ability to display different epitopes, which may alter antibody recognition and binding affinity (Fig. 6B and C). Taking the data together, we conclude that the incomplete neutralization phenotype and potency of neutralization can be independently influenced by the YXXL motif in examining HIV infections with cell-associated viruses.

DISCUSSION

Studies that compare the levels of neutralization of cell-free and cell-associated forms of HIV-1 have generally found that cell-associated virus requires higher concentrations of antibody to achieve equivalent levels of neutralization (1, 3–5, 7–10, 55). This reduced sensitivity to neutralization has been observed with different viral isolates to various degrees, depending upon the antibody (7). Thus far, however, the maximum

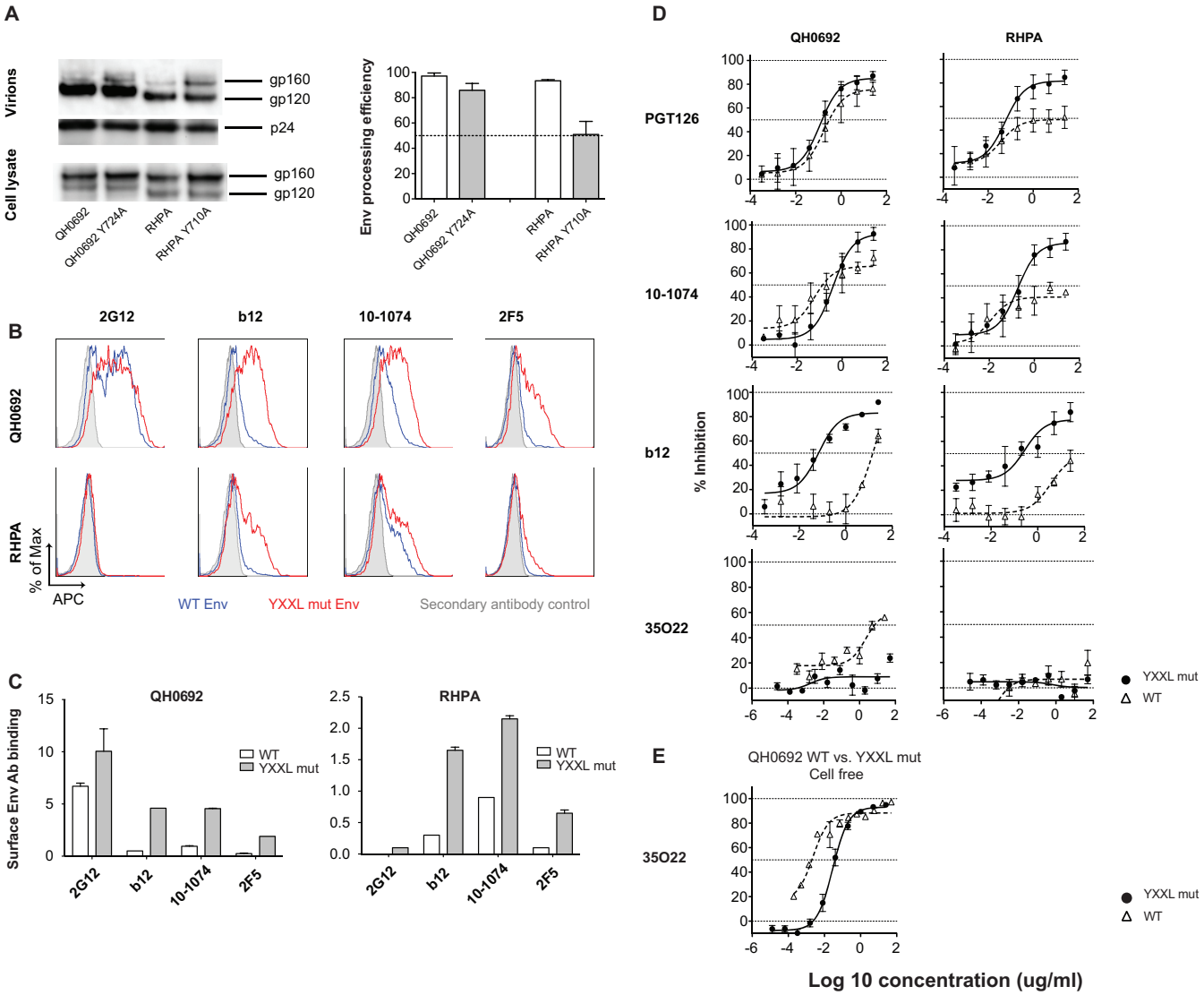

FIG 6 Impact of mutation of the YXXL sorting motif on potency of antibody neutralization and maximum neutralization phenotype in both cell-associated and cell-free infection. (A) NLCI constructs with wild-type and YXXL mutant Env expression in transfected 293T cells and Env incorporation into viral particles were examined by Western blotting. The amount of sample loaded was normalized to the amount of p24 antigen as determined by ELISA. The processing efficiency of Env precursor gp160 was quantitated, and the data are shown in bar graphs. Error bars represent SEM of results from duplicates of at least two independent experiments conducted on different dates. (B) Jurkat cells were nucleofected with $NLCI_{QH0692\text{-}Y724A}$, $NLCI_{RHPA\text{-}Y710A}$, $NLCI_{QH0692}$, and $NLCI_{RHPA}$, and at 24 h after neucleofection, cells were stained for analysis of surface Env expression levels with MAb 2G12, b12, 10-1074, and 2F5 followed by Alexa Fluor 647 anti-human IgG. Gray shades in histograms represent secondary antibody control; blue and red lines represent wild-type strain and YXXL mutant (mut) surface Env staining, respectively. APC, allophycocyanin. (C) Surface Env binding with MAbs 2G12, b12, 10-1074, and 2F5 represented by the relative values of MFI, which is a ratio of the median MFI determined for Env-AF647 of mCherry-high cells to the MFI of secondary antibody control and was calculated as follows: relative MFI = (MFI Env-AF647 − MFI secondary antibody control)/MFI secondary antibody control. The relative values of MFI of the WT strain and YXXL mutants stained with different MAbs are shown in white and gray, respectively. (D) Mutants with a disrupted YXXL motif were tested for maximal percentage of inhibition by MAbs PGT126, 10-1074, b12, and 35O22 in cell-to-cell neutralization. (E) The WT strain and a YXXL mutant of $NLCI_{QH0692}$ were tested and compared for neutralization sensitivity in cell-free infection with 35O22.

neutralization achieved with saturating concentrations of antibody has not been carefully scrutinized against T/F Envs.

Here we utilized a $CD4^+$ T cell-to-T cell transmission assay with T/F Env-carrying molecular clones that express Env within a native proviral context using a flow cytometry-based assay that can detect individual infection events with exceptionally low background and a wide dynamic range (4, 56, 57). The T cell-to-T cell system used here is more physiologically relevant than systems that use nonlymphoid virus producer cells such as 293T cells. This study allowed us to assess a critical parameter, i.e., the maximum efficacy that can be achieved with saturating concentrations of bNAbs in blocking cell-associated HIV.

Examining a panel of bNAbs targeting different epitopes against the two T/F Env-expressing viruses, we observed surprisingly wide gaps in the abilities of these antibodies to neutralize cell-associated virus compared to cell-free forms with respect to both potency and maximum efficacy. Consistent with prior studies (7), we observed that the potency of bNAbs against HIV-1 cell-to-cell transmission is frequently decreased in comparison to that seen with cell-free virus in an epitope- and viral strain-dependent manner. The magnitude of the difference in IC_{50} levels between cell-associated and cell-free infections ranged as illustrated in the heat map representation of the panel of antibodies (Fig. 4A). In assays of the antibodies targeting different epitopes, including the CD4bs, MPER, glycan-dependent V3, and gp120/gp41 interface, each was associated with a higher IC_{50} with cell-associated than with cell-free virus, and yet the magnitudes of this shift differed for all of the antibodies. The largest IC_{50} difference in cell-to-cell neutralization over cell-free neutralization was an approximately 3,400-fold change for QH0692 Env targeted by gp120/gp41 interface antibody 35O22, while the fold difference in IC_{50} seen with PGT121 for the same Env was as low as 1.9. In addition, the magnitudes of IC_{50} differences also ranged among different viruses. Despite the extraordinary reduction in the potency of inhibition of cell-to-cell infection compared to cell-free infection of 35O22 noted with QH0692 Env, the same antibody displayed only a 7.3-fold IC_{50} difference with $NLCI_{NL4-3}$ in cell-to-cell infection over cell-free infection.

Importantly, we found that the neutralization resistance of cell-associated HIV-1 was reflected not only in reduced IC_{50}s but also in decreases in the maximal inhibition of cell-to-cell infection. In many cases, we observed an inability of bNAbs to completely neutralize the virus at high antibody concentrations that was unique to cell-to-cell infection and not seen with infection by cell-free virus. In a severe case, we observed incomplete inhibition where the peak neutralization blocked only 36% of the infection (Fig. 4B). Incomplete neutralization of cell-associated virus was observed using CD4bs antibody HJ16 with RHPA (Fig. 3C), MPER antibody 2F5 with RHPA (Fig. 3D), MPER antibody 4E10 with QH0692 (Fig. 3D), and glycan-dependent V3 MAbs PGT121, PGT126, and 10-1074 with both QH0692 and RHPA (Fig. 3G). These results indicate that a significant fraction of cell-associated virus can be completely resistant to neutralizing antibodies even at saturating concentrations. Neutralizing epitopes that are displayed on cell-free Env may be less accessible or completely absent on a fraction of cell-associated Env. Since the fraction of resistant virus can be very high, the maximum neutralization threshold may represent a facile means of viral escape even in the presence of high titers of neutralizing antibodies through cell-to-cell infection. This possibility suggests that "efficacy," or maximum neutralization, is a critical parameter to consider in addition to antibody potency. Certain potent antibodies that inhibit cell-free infection very efficiently may fail to completely block cell-to-cell transmission even at saturating concentrations, potentially contributing to a lack of viral control in antibody therapy. The diminished neutralization potency and efficacy of certain bNAbs against HIV-1 cell-to-cell infection observed here are dependent upon viral sequences as well as epitope targets. Certain bNAbs such as PGT121 are capable of controlling viremia in nonhuman primate models (38), while we have also observed that these can display incomplete neutralization against certain clones. It will be interesting to determine whether the efficacy of these antibodies against cell-associated virus inoculums correlates with their ability to inhibit simian immunodeficiency virus (SIV) *in vivo*.

Interestingly, the maximum neutralization phenotype was more evident with T/F Envs than with the laboratory-adapted NL4-3 and chronic viral strain JR-FL Envs, which could be attributed to different transition dynamics between conformational states for laboratory strains and T/F viruses. Laboratory-adapted Envs, like NL4-3 Env, are suggested to be conformationally more flexible, exhibiting a more frequently spontaneous transition between "closed" and "open" conformations (58). Env of T/F viruses may spend more time in a closed conformation, occluding some neutralizing epitopes and restricting antibody accessibility. Our results indicate that these properties may be influenced by the environment of Env on the cell surface or the virion surface.

The Burton group recently described incomplete neutralization in cell-free infection, particularly with glycan-dependent and glycan-related epitopes. In most cases, the neutralization plateau that they observed was between 90% and 100% (50). In our study, the cell-free viruses that we tested were inhibited at levels of up to 95% in most cases, while we observed cases of cell-to-cell infection where the maximum inhibition level was as low as 36%. On the basis of the results presented here, it is unlikely that the poor maximum neutralization phenotypes observed in cell-to-cell infection were solely due to cell type-dependent differences, although we note that we did also observe instances of cell type-specific differences in potency (Fig. 5A).

One possible phenotypic difference between the producer cells that potentially contributes to the cell type-dependent shifts in IC_{50} observed between cell-free viruses produced from different cell lines is that of glycosylation heterogeneity. Kif treatment resulted in decreased IC_{50}s in both cell-free infection (59, 60) and cell-to-cell infection (Fig. 5C) and in a very minor increase in maximum neutralization in cell-to-cell infection. This result further indicates that potency and efficacy are two important and independent parameters to consider in antibody therapy against HIV-1.

The precise mechanism responsible for cell-to-cell infection being more resistant to neutralization than cell-free infection remains unclear. A revealing study demonstrated that a truncation mutation of the CT not only increased Env expression on the surface of HIV-1-infected cells but also significantly enhanced neutralization of cell-to-cell infection, suggesting that the CT of gp41 plays an important role in regulating exposure of key neutralizing epitopes during HIV-1 cell-to-cell infection (3). Several domains of CT have been identified as differentially regulating cell-free and cell-to-cell infections (48). Specific sequences or structural motifs have been identified as regulating endocytosis of Env, thus modulating fusion activity, antibody binding, and neutralization sensitivity (44, 46, 61, 62). The maximum efficacy observed in cell-to-cell transmission of HIV-1 carrying T/F Envs can also be influenced by a motif within the CT of gp41. When the membrane-proximal internal tyrosine-based sorting signal YXXL was mutated, we found in assays of the $NLCI_{QH0692}$ YXXL mutant that the maximum neutralization of cell-associated HIV-1 increased in PGT126, 10-1074, and b12 and decreased in 35O22. This further indicates that this motif can modulate cell surface Env in a manner that changes the potency and maximum efficacy of bNAbs, particularly during HIV-1 cell-to-cell transmission. We noted that with the V3 glycan antibodies PGT126 and 10-1074, the increase in maximum neutralization of the YXXL mutant occurred without a large shift in the IC_{50} with $NLCI_{QH0692}$, whereas increases in both potency and maximum neutralization were observed with b12. This further indicates that potency and maximum efficacy are distinct properties that can both be influenced by changes in the Env CT.

YXXL mutation was also reported to affect polarization of Gag and to compromise cell-to-cell transmission efficiency (63). In our assays, the YXXL mutants exhibited about 50% lower cell-to-cell transmission efficiency than their wild-type counterparts (data not shown), which is consistent with a previous report (63). We speculate that the YXXL mutation can alter the conformational state of the CT or change intracellular interactions between the CT and other cellular machinery. These changes may cause allosteric conformational changes in Env ectodomain that in turn impact virus transmission efficiency or its sensitivity to neutralizing antibodies.

HIV-infected cells maintain low copy numbers of Env on their surface by rapid endocytosis and the activity of endosomal recycling machinery (52–54, 64–66). When the Env recycling pathway is blocked by disrupting the tyrosine-based YXXL sorting motif, Env accumulates on the cell surface, as can be detected by increased binding with different MAbs (Fig. 6B). Based on the results of staining of infected cells with 2G12 (a glycan-reactive antibody that may be less sensitive to Env conformation change), the YXXL mutation increased surface Env to a lesser extent than a full CT truncation (3, 47, 48). However, in these studies, it is challenging to distinguish between increased cell-surface Env expression and enhanced epitope exposure. We observed that the fold changes in levels of antibody binding to surface Env with or without the YXXL mutation

differed among MAbs targeting different epitopes (Fig. 6C). The increased levels of binding of these conformationally sensitive MAbs to Env with the YXXL mutation indicate that, in addition to increases in Env surface levels, the overall conformation of Env may also be affected. These differences can either increase or decrease cell-to-cell neutralization sensitivity in a manner that does not correlate with the total amount of Env (Fig. 6C). The antibodies may therefore recognize different states of Env with different levels of affinity. A proposed nuclear magnetic resonance (NMR) structure identified the tyrosine-based YXXL sorting signal as being located within a hydrophilic core of transmembrane domain (TMD) of gp41, contributing to stabilize the trimeric structure TMD. Mutation of this motif is suggested to destabilize the hydrophilic core of TMD trimer, altering the antigenic surfaces of the ectodomain of gp120 (67). Thus, an attractive model to explain the changes in the neutralization sensitivity of the YXXL mutant viruses is that this membrane-proximal internal motif is involved in allosteric modulation of gp120.

On the basis of the presented results, we are attracted to a model whereby engagement of Env in recycling pathways can modulate conformational states of gp120. We further speculate that incomplete neutralization may allow HIV-1 to evade certain neutralizing responses by spreading through cell-to-cell pathways. When pursuing success in therapeutic antibody strategies, both the potency and the efficacy of antibodies against cell-free and cell-associated pathways should be considered. Future studies are needed to elucidate the changes in the Env state that allow changes in potency or efficacy.

MATERIALS AND METHODS

Viral constructs. Full-length clade B primary isolate transmitted/founder (T/F) HIV-1 Env QH0692 and RHPA (B. H. Hahn and J. F. Salazar-Gonzalez; B. H. Hahn, X. Wei, and G. M. Shaw; ARP catalog no. 11227) were cloned into the pNL4-3-based $NLCI_{NL4-3}$ backbone in place of NL4-3 Env (68). $NLCI_{NL4-3}$ is a proviral molecular clone with mCherry in the *nef* locus. Nef expression is restored by use of the internal ribosome entry site (IRES) (69). $NLCI_{JR-FL}$ was generated using full-length JR-FL Env, a chronic CCR5-tropic Env. Single amino acid mutations were introduced into $NLCI_{QH0692}$ and $NLCI_{RHPA}$ to generate YXXL motif mutants. All constructs were generated using overlap PCR with restriction enzymes EcoRI and MluI. PCR-amplified sequences were verified by Sanger sequencing.

Cells and cell culture. Cells from the human cell line Jurkat E6-1 were obtained from Arthur Weiss through the NIH ARP. Cells were maintained in RPMI 1640 medium supplemented with 10% fetal bovine serum (FBS), 100 U/ml penicillin, 100 μg/ml streptomycin, and 2 mM glutamine (complete RPMI medium) and were passaged regularly and maintained at a density below 1×10^6/ml. The MT4R5 cell line was obtained from James E. Robinson and was cultured in complete RPMI medium supplemented with 2 μg/ml puromycin. The 293T and TZM-bl cell lines were obtained from ATCC and the ARP (catalog no. 8129) and maintained in Dulbecco's modified Eagle medium (DMEM) with 10% fetal bovine serum (FBS), 100 U/ml penicillin, 100 μg/ml streptomycin, and 2 mM glutamine.

Broadly neutralizing monoclonal antibody (bNAbs) and HIV-1-positive patient IgG. A panel of bNAbs targeting different epitopes on HIV-1 Env were tested for their ability to block HIV-1 cell-free and cell-to-cell infections. Unless otherwise stated, the following antibodies were tested in 3-fold serial dilutions starting at the highest concentration indicated in both cell-free and cell-to-cell neutralization assays: anti-CD4 MAb leu3a (BD Biosciences) (0.5 μg/ml); CD4bs MAb VRC01 (John Mascola, ARP) (25 μg/ml); CD4bs MAb HJ16 (Antonio Lanzavecchia, ARP) (50 μg/ml); anti-V1V2 Apex MAb PG9 (International AIDS Vaccine Initiative [IAVI], ARP) (50 μg/ml); anti-V3 MAb PGT121 (IAVI, ARP) (50 μg/ml); PGT126 (IAVI, ARP) (50 μg/ml) and 10-1074 (50 μg/ml) (Michel C. Nussenzweig, ARP); anti-gp41 MAbs 2F5 and 4E10 (Hermann Katinger, ARP) (50 μg/ml); anti-gp120/gp41 interface MAb 35O22 (Jinghe Huang and Mark Connors, ARP) (50 μg/ml); and anti-gp120 glycan MAb 2G12 (Hermann Katinger, ARP) (100 μg/ml). Pooled HIV-1-positive patient IgG (HIVIG) (Luiz Barbosa, ARP) was tested at a starting concentration of 50 μg/ml. Neutralizing HIV-1 patient plasma samples were obtained through the Jack Martin Fund Clinic of Mount Sinai Hospital following an Institutional Review Board (IRB)-approved protocol. Patient IgG was isolated by affinity purification using protein A/G beads (Thermo Fisher Scientific).

Cell-free infection and neutralization assay. Cell-free virus particles were produced by transfection of 293T cells using Polyjet (SignaGen) or by nucleofection of Jurkat cells (Amaxa Biosystems) with plasmid DNA from NLCI-based primary isolates. Cell-free virus particles were harvested 48 h after transfection of 293T cells, centrifuged at $1,000 \times g$, filtered with a membrane with a pore size of 0.45 μm, and stored in a −80°C freezer. Virus supernatant was harvested from nucleofected Jurkat cells 72 h after nucleofection. For cell-free infection assays, the viral inoculum was normalized to p24 to infect 1.25×10^5 CCR5-expressing T cells in flat-bottom 96-well plates. In the presence of neutralizing antibodies or HIV-1-positive patient IgG, viral supernatant was preincubated with equal volumes of medium containing MAb at 37°C for 30 min before mixing with MT4R5 cells was performed. In the case of anti-CD4 antibody

Leu3a, equal volumes of medium containing antibody were preincubated with target cells before mixing with viral supernatant was performed.

To ensure measurement of a single round of infection, medium was replaced at 18 h postinfection with fresh medium containing 10 μM azidothymidine (AZT; ARP). At 48 h postinfection, cells were treated with tryspin-EDTA to remove surface-attaching viral particles, neutralized with complete RPMI medium, washed with phosphate-buffered saline (PBS), and fixed with 2% paraformaldehyde. Fluorescence signal from infected cells was detected by flow cytometry using a BD LSRFortessa flow cytometer (BD Biosciences) and analyzed with Flowjo (Tree Star, Inc.).

Cell-to-cell infection and neutralization assay. A cell-associated viral inoculum was provided by the use of Jurkat cells nucleofected (Amaxa Biosystems) with the panel of NLCI constructs that carried primary isolate Envs. Nucleofected donor cells were cultured overnight, after which dead cells were removed by Ficoll-Paque density gradient centrifugation. Nucleofected donor Jurkat cells and target CCR5-expressing CD4$^+$ T cells were subjected to dye labeling with 5 μM cell proliferation dye eFluor 670 (eBiosciences) and 10 μM cell proliferation dye eFluor 450 (eBiosciences), respectively. At the time of coculture, the percentages of HIV-expressing donor cells were adjusted to similar fractions for all cells by adjusting the amount of DNA used in nucleofection or by diluting the donor cells with nonnucleofected Jurkat cells. Donor cells (1.25×10^5) were cocultured with same number of HIV-1 naive target cells in each well of round bottom 96-well plates. In the presence of neutralizing antibodies or HIV-1-positive patient IgG, donor cells were preincubated with equal volumes of antibody-containing medium at 37°C for 30 min before mixing with MT4R5 cells was performed. In the case of anti-CD4 antibody Leu3a, equal volumes of medium containing antibody were preincubated with target cells before mixing with nucleofected donor cells was performed. For single-round infection, medium was replaced with fresh medium containing 10 μM AZT about 18 h after the coculture. At 40 to 48 h postinfection, cells were treated with trypsin-EDTA to remove surface-attaching viral particles and to disrupt donor-target doublets. Cells were then neutralized with complete RPMI medium, washed with PBS, and fixed with 2% paraformaldehyde. Samples were then analyzed using a LSRFortessa flow cytometer (BD Biosciences) and Flowjo (Tree Star, Inc.).

Transwell assay. Nucleofected Jurkat donor cells were prepared as described for the cell-to-cell infection assay. Amaxa nucleofected and eFluor 670-labeled donor cells (5×10^5) were placed in a transwell chamber. The same number of eFluor 450-labeled MT4R5 target cells was placed in the bottom wells of a 24-well plate. A membrane with a pore size of 0.4 μm that separated the two compartments prevented cell-cell contact between donor and target cells without inhibiting the free passage of virus particles. AZT (10 μM) was added 18 h after the coculture. Samples were harvested 40 h after coculture for fluorescence-activated cell sorter (FACS) analysis.

Western blotting. Virus supernatant was collected from transfected 293T cells and quantitated by p24 enzyme-linked immunosorbent assay (ELISA). Virus was pelleted by ultracentrifugation through 6% OptiPrep density gradient medium (Sigma-Aldrich), resuspended in PBS, and quantitated by p24 ELISA. Both concentrated virus and transfected 293T cells were lysed with 1% Tris–Triton lysis buffer supplemented with 1× protease inhibitor (Roche). Lysed 293T cells were centrifuged at 13,000 rpm for 3 min at 4°C. The total protein concentration in cell lysates was determined by the use of a Coomassie Plus assay kit (Thermo Scientific). Cell lysates and viral particle lysates were normalized according to protein concentration and p24 amount, respectively. All samples were denatured and reduced before being separated by sodium dodecyl sulfate polyacrylamide gel electrophoresis (SDS-PAGE). Protein was transferred to a polyvinylidene difluoride (PVDF) membrane (GE Healthcare) for antibody detection. Polyclonal sheep anti-gp120 antibody (Michael Phelan, ARP) was used to probe gp120 and gp160; pooled clade B HIV-1-infected patient IgG was used to probe all HIV-1 viral proteins (Luiz Barbosa, ARP). Horseradish peroxidase (HRP)-conjugated anti-sheep or anti-human antibodies (Jackson ImmunoResearch Laboratories, Inc.) were used as secondary antibodies. Chemiluminescence signal was detected by the use of SuperSignal West Femto maximum-sensitivity substrate (ThermoFisher Scientific) and visualized using a FluorChem E imaging system (ProteinSimple). Signal intensity was quantitated with Image J (Wayne Rasband, National Institutes of Health).

Surface Env MAb staining. Jurkat cells were nucleofected with T/F Envs carrying NLCI constructs in cell-to-cell infection assays as described previously. Viable cells were separated by Ficoll gradient centrifugation, washed, placed into a V-bottom 96-well plate at a density of 1.5×10^5 per well, and stained with 10 μg/ml HIV-1 monoclonal antibody 2G12 at 4°C for 45 min followed by 2 μg/ml Alexa Fluor 647 (AF647)-conjugated goat anti-human IgG (Life Technologies) at 4°C for 30 min. Cells were also stained with 5 μg/ml HIV-1 MAb b12, 10-1074, or 2F5 (ARP) at 4°C for 45 min followed by 2 μg/ml AF647-conjugated goat anti-human IgG (Life Technologies) at 4°C for 30 min. Samples were then washed and fixed for FACS analysis. Average median fluorescence intensity levels were calculated from two independent experiments.

To quantitate cell-surface Env expression levels, we examined the mean fluorescence intensity (MFI) of mCherry-high populations, corresponding to HIV-1-infected cells that express both early and late HIV-1 genes, including the Env gene. The level of surface Env binding by each anti-HIV MAb was calculated as the relative MFI value, which represents a ratio of the MFI of Env-AF647 to that of a secondary antibody-alone control, as follows: relative MFI = (MFI of Env-AF647 − MFI of secondary antibody control)/MFI of secondary antibody control alone.

ACKNOWLEDGMENTS

We thank members of the B. K. Chen laboratory for helpful comments and advice and acknowledge the Flow Cytometry Shared Resource Facility from the Immunology

Institute of the Icahn School of Medicine at Mount Sinai and the Mount Sinai Core Facility.

This work was supported by GM113885, AI104471, AI112423, and F31GM116650 from the National Institutes of Health.

We declare that we have no conflicting financial interests.

REFERENCES

1. Chen P, Hubner W, Spinelli MA, Chen BK. 2007. Predominant mode of human immunodeficiency virus transfer between T cells is mediated by sustained Env-dependent neutralization-resistant virological synapses. J Virol 81:12582–12595. https://doi.org/10.1128/JVI.00381-07.
2. Sourisseau M, Sol-Foulon N, Porrot F, Blanchet F, Schwartz O. 2007. Inefficient human immunodeficiency virus replication in mobile lymphocytes. J Virol 81:1000–1012. https://doi.org/10.1128/JVI.01629-06.
3. Durham ND, Yewdall AW, Chen P, Lee R, Zony C, Robinson JE, Chen BK. 2012. Neutralization resistance of virological synapse-mediated HIV-1 Infection is regulated by the gp41 cytoplasmic tail. J Virol 86:7484–7495. https://doi.org/10.1128/JVI.00230-12.
4. Malbec M, Porrot F, Rua R, Horwitz J, Klein F, Halper-Stromberg A, Scheid JF, Eden C, Mouquet H, Nussenzweig MC, Schwartz O. 2013. Broadly neutralizing antibodies that inhibit HIV-1 cell to cell transmission. J Exp Med 210:2813–2821. https://doi.org/10.1084/jem.20131244.
5. Abela IA, Berlinger L, Schanz M, Reynell L, Gunthard HF, Rusert P, Trkola A. 2012. Cell-cell transmission enables HIV-1 to evade inhibition by potent CD4bs directed antibodies. PLoS Pathog 8:e1002634. https://doi.org/10.1371/journal.ppat.1002634.
6. Sigal A, Kim JT, Balazs AB, Dekel E, Mayo A, Milo R, Baltimore D. 2011. Cell-to-cell spread of HIV permits ongoing replication despite antiretroviral therapy. Nature 477:95–98. https://doi.org/10.1038/nature10347.
7. Reh L, Magnus C, Schanz M, Weber J, Uhr T, Rusert P, Trkola A. 2015. Capacity of broadly neutralizing antibodies to inhibit HIV-1 cell-cell transmission is strain- and epitope-dependent. PLoS Pathog 11:e1004966. https://doi.org/10.1371/journal.ppat.1004966.
8. Martin N, Welsch S, Jolly C, Briggs JA, Vaux D, Sattentau QJ. 2010. Virological synapse-mediated spread of human immunodeficiency virus type 1 between T cells is sensitive to entry inhibition. J Virol 84:3516–3527. https://doi.org/10.1128/JVI.02651-09.
9. Gombos RB, Kolodkin-Gal D, Eslamizar L, Owuor JO, Mazzola E, Gonzalez AM, Korioth-Schmitz B, Gelman RS, Montefiori DC, Haynes BF, Schmitz JE. 2015. Inhibitory effect of individual or combinations of broadly neutralizing antibodies and antiviral reagents against cell-free and cell-to-cell HIV-1 transmission. J Virol 89:7813–7828. https://doi.org/10.1128/JVI.00783-15.
10. Duncan CJ, Williams JP, Schiffner T, Gartner K, Ochsenbauer C, Kappes J, Russell RA, Frater J, Sattentau QJ. 2014. High-multiplicity HIV-1 infection and neutralizing antibody evasion mediated by the macrophage-T cell virological synapse. J Virol 88:2025–2034. https://doi.org/10.1128/JVI.03245-13.
11. Massanella M, Puigdomenech I, Cabrera C, Fernandez-Figueras MT, Aucher A, Gaibelet G, Hudrisier D, Garcia E, Bofill M, Clotet B, Blanco J. 2009. Antigp41 antibodies fail to block early events of virological synapses but inhibit HIV spread between T cells. AIDS 23:183–188. https://doi.org/10.1097/QAD.0b013e32831ef1a3.
12. Jolly C, Kashefi K, Hollinshead M, Sattentau QJ. 2004. HIV-1 cell to cell transfer across an Env-induced, actin-dependent synapse. J Exp Med 199:283–293. https://doi.org/10.1084/jem.20030648.
13. Puigdomènech I, Massanella M, Izquierdo-Useros N, Ruiz-Hernandez R, Curriu M, Bofill M, Martinez-Picado J, Juan M, Clotet B, Blanco J. 2008. HIV transfer between CD4 T cells does not require LFA-1 binding to ICAM-1 and is governed by the interaction of HIV envelope glycoprotein with CD4. Retrovirology 5:32. https://doi.org/10.1186/1742-4690-5-32.
14. Ruggiero E, Bona R, Muratori C, Federico M. 2008. Virological consequences of early events following cell-cell contact between human immunodeficiency virus type 1-infected and uninfected $CD4^+$ cells. J Virol 82:7773–7789. https://doi.org/10.1128/JVI.00695-08.
15. Bosch B, Grigorov B, Senserrich J, Clotet B, Darlix JL, Muriaux D, Este JA. 2008. A clathrin-dynamin-dependent endocytic pathway for the uptake of HIV-1 by direct T cell-T cell transmission. Antiviral Res 80:185–193. https://doi.org/10.1016/j.antiviral.2008.06.004.
16. Hübner W, McNerney GP, Chen P, Dale BM, Gordon RE, Chuang FY, Li XD, Asmuth DM, Huser T, Chen BK. 2009. Quantitative 3D video microscopy of HIV transfer across T cell virological synapses. Science 323:1743–1747. https://doi.org/10.1126/science.1167525.
17. Blanco J, Bosch B, Fernandez-Figueras MT, Barretina J, Clotet B, Este JA. 2004. High level of coreceptor-independent HIV transfer induced by contacts between primary CD4 T cells. J Biol Chem 279:51305–51314. https://doi.org/10.1074/jbc.M408547200.
18. Dale BM, McNerney GP, Thompson DL, Hubner W, de Los Reyes K, Chuang FY, Huser T, Chen BK. 2011. Cell-to-cell transfer of HIV-1 via virological synapses leads to endosomal virion maturation that activates viral membrane fusion. Cell Host Microbe 10:551–562. https://doi.org/10.1016/j.chom.2011.10.015.
19. Walker LM, Phogat SK, Chan-Hui PY, Wagner D, Phung P, Goss JL, Wrin T, Simek MD, Fling S, Mitcham JL, Lehrman JK, Priddy FH, Olsen OA, Frey SM, Hammond PW; Protocol G Principal Investigators, Kaminsky S, Zamb T, Moyle M, Koff WC, Poignard P, Burton DR. 2009. Broad and potent neutralizing antibodies from an African donor reveal a new HIV-1 vaccine target. Science 326:285–289. https://doi.org/10.1126/science.1178746.
20. Wu X, Yang ZY, Li Y, Hogerkorp CM, Schief WR, Seaman MS, Zhou T, Schmidt SD, Wu L, Xu L, Longo NS, McKee K, O'Dell S, Louder MK, Wycuff DL, Feng Y, Nason M, Doria-Rose N, Connors M, Kwong PD, Roederer M, Wyatt RT, Nabel GJ, Mascola JR. 2010. Rational design of envelope identifies broadly neutralizing human monoclonal antibodies to HIV-1. Science 329:856–861. https://doi.org/10.1126/science.1187659.
21. Bonsignori M, Hwang KK, Chen X, Tsao CY, Morris L, Gray E, Marshall DJ, Crump JA, Kapiga SH, Sam NE, Sinangil F, Pancera M, Yongping Y, Zhang B, Zhu J, Kwong PD, O'Dell S, Mascola JR, Wu L, Nabel GJ, Phogat S, Seaman MS, Whitesides JF, Moody MA, Kelsoe G, Yang X, Sodroski J, Shaw GM, Montefiori DC, Kepler TB, Tomaras GD, Alam SM, Liao HX, Haynes BF. 2011. Analysis of a clonal lineage of HIV-1 envelope V2/V3 conformational epitope-specific broadly neutralizing antibodies and their inferred unmutated common ancestors. J Virol 85:9998–10009. https://doi.org/10.1128/JVI.05045-11.
22. Huang J, Ofek G, Laub L, Louder MK, Doria-Rose NA, Longo NS, Imamichi H, Bailer RT, Chakrabarti B, Sharma SK, Alam SM, Wang T, Yang Y, Zhang B, Migueles SA, Wyatt R, Haynes BF, Kwong PD, Mascola JR, Connors M. 2012. Broad and potent neutralization of HIV-1 by a gp41-specific human antibody. Nature 491:406–412. https://doi.org/10.1038/nature11544.
23. Morris L, Chen X, Alam M, Tomaras G, Zhang R, Marshall DJ, Chen B, Parks R, Foulger A, Jaeger F, Donathan M, Bilska M, Gray ES, Abdool Karim SS, Kepler TB, Whitesides J, Montefiori D, Moody MA, Liao HX, Haynes BF. 2011. Isolation of a human anti-HIV gp41 membrane proximal region neutralizing antibody by antigen-specific single B cell sorting. PLoS One 6:e23532. https://doi.org/10.1371/journal.pone.0023532.
24. Corti D, Langedijk JP, Hinz A, Seaman MS, Vanzetta F, Fernandez-Rodriguez BM, Silacci C, Pinna D, Jarrossay D, Balla-Jhagjhoorsingh S, Willems B, Zekveld MJ, Dreja H, O'Sullivan E, Pade C, Orkin C, Jeffs SA, Montefiori DC, Davis D, Weissenhorn W, McKnight A, Heeney JL, Sallusto F, Sattentau QJ, Weiss RA, Lanzavecchia A. 2010. Analysis of memory B cell responses and isolation of novel monoclonal antibodies with neutralizing breadth from HIV-1-infected individuals. PLoS One 5:e8805. https://doi.org/10.1371/journal.pone.0008805.
25. Scheid JF, Mouquet H, Ueberheide B, Diskin R, Klein F, Oliveira TY, Pietzsch J, Fenyo D, Abadir A, Velinzon K, Hurley A, Myung S, Boulad F, Poignard P, Burton DR, Pereyra F, Ho DD, Walker BD, Seaman MS, Bjorkman PJ, Chait BT, Nussenzweig MC. 2011. Sequence and structural convergence of broad and potent HIV antibodies that mimic CD4 binding. Science 333:1633–1637. https://doi.org/10.1126/science.1207227.
26. Liao HX, Lynch R, Zhou T, Gao F, Alam SM, Boyd SD, Fire AZ, Roskin KM, Schramm CA, Zhang Z, Zhu J, Shapiro L; NISC Comparative Sequencing Program, Mullikin JC, Gnanakaran S, Hraber P, Wiehe K, Kelsoe G, Yang

G, Xia SM, Montefiori DC, Parks R, Lloyd KE, Scearce RM, Soderberg KA, Cohen M, Kamanga G, Louder MK, Tran LM, Chen Y, Cai F, Chen S, Moquin S, Du X, Joyce MG, Srivatsan S, Zhang B, Zheng A, Shaw GM, Hahn BH, Kepler TB, Korber BT, Kwong PD, Mascola JR, Haynes BF. 2013. Co-evolution of a broadly neutralizing HIV-1 antibody and founder virus. Nature 496:469–476. https://doi.org/10.1038/nature12053.

27. Zhu Z, Qin HR, Chen W, Zhao Q, Shen X, Schutte R, Wang Y, Ofek G, Streaker E, Prabakaran P, Fouda GG, Liao HX, Owens J, Louder M, Yang Y, Klaric KA, Moody MA, Mascola JR, Scott JK, Kwong PD, Montefiori D, Haynes BF, Tomaras GD, Dimitrov DS. 2011. Cross-reactive HIV-1-neutralizing human monoclonal antibodies identified from a patient with 2F5-like antibodies. J Virol 85:11401–11408. https://doi.org/10.1128/JVI.05312-11.
28. Walker LM, Huber M, Doores KJ, Falkowska E, Pejchal R, Julien JP, Wang SK, Ramos A, Chan-Hui PY, Moyle M, Mitcham JL, Hammond PW, Olsen OA, Phung P, Fling S, Wong CH, Phogat S, Wrin T, Simek MD; Protocol G Principal Investigators, Koff WC, Wilson IA, Burton DR, Poignard P. 2011. Broad neutralization coverage of HIV by multiple highly potent antibodies. Nature 477:466–470. https://doi.org/10.1038/nature10373.
29. Pejchal R, Doores KJ, Walker LM, Khayat R, Huang PS, Wang SK, Stanfield RL, Julien JP, Ramos A, Crispin M, Depetris R, Katpally U, Marozsan A, Cupo A, Maloveste S, Liu Y, McBride R, Ito Y, Sanders RW, Ogohara C, Paulson JC, Feizi T, Scanlan CN, Wong CH, Moore JP, Olson WC, Ward AB, Poignard P, Schief WR, Burton DR, Wilson IA. 2011. A potent and broad neutralizing antibody recognizes and penetrates the HIV glycan shield. Science 334:1097–1103. https://doi.org/10.1126/science.1213256.
30. Huang J, Kang BH, Pancera M, Lee JH, Tong T, Feng Y, Imamichi H, Georgiev IS, Chuang GY, Druz A, Doria-Rose NA, Laub L, Sliepen K, van Gils MJ, de la Pena AT, Derking R, Klasse PJ, Migueles SA, Bailer RT, Alam M, Pugach P, Haynes BF, Wyatt RT, Sanders RW, Binley JM, Ward AB, Mascola JR, Kwong PD, Connors M. 2014. Broad and potent HIV-1 neutralization by a human antibody that binds the gp41-gp120 interface. Nature 515:138–142. https://doi.org/10.1038/nature13601.
31. Klein F, Gaebler C, Mouquet H, Sather DN, Lehmann C, Scheid JF, Kraft Z, Liu Y, Pietzsch J, Hurley A, Poignard P, Feizi T, Morris L, Walker BD, Fatkenheuer G, Seaman MS, Stamatatos L, Nussenzweig MC. 2012. Broad neutralization by a combination of antibodies recognizing the CD4 binding site and a new conformational epitope on the HIV-1 envelope protein. J Exp Med 209:1469–1479. https://doi.org/10.1084/jem.20120423.
32. Mouquet H, Klein F, Scheid JF, Warncke M, Pietzsch J, Oliveira TY, Velinzon K, Seaman MS, Nussenzweig MC. 2011. Memory B cell antibodies to HIV-1 gp140 cloned from individuals infected with clade A and B viruses. PLoS One 6:e24078. https://doi.org/10.1371/journal.pone.0024078.
33. Shingai M, Nishimura Y, Klein F, Mouquet H, Donau OK, Plishka R, Buckler-White A, Seaman M, Piatak M, Jr, Lifson JD, Dimitrov DS, Nussenzweig MC, Martin MA. 2013. Antibody-mediated immunotherapy of macaques chronically infected with SHIV suppresses viraemia. Nature 503:277–280.
34. Shingai M, Donau OK, Plishka RJ, Buckler-White A, Mascola JR, Nabel GJ, Nason MC, Montefiori D, Moldt B, Poignard P, Diskin R, Bjorkman PJ, Eckhaus MA, Klein F, Mouquet H, Cetrulo Lorenzi JC, Gazumyan A, Burton DR, Nussenzweig MC, Martin MA, Nishimura Y. 2014. Passive transfer of modest titers of potent and broadly neutralizing anti-HIV monoclonal antibodies block SHIV infection in macaques. J Exp Med 211:2061–2074. https://doi.org/10.1084/jem.20132494.
35. Hessell AJ, Poignard P, Hunter M, Hangartner L, Tehrani DM, Bleeker WK, Parren PW, Marx PA, Burton DR. 2009. Effective, low-titer antibody protection against low-dose repeated mucosal SHIV challenge in macaques. Nat Med 15:951–954. https://doi.org/10.1038/nm.1974.
36. Hessell AJ, Rakasz EG, Poignard P, Hangartner L, Landucci G, Forthal DN, Koff WC, Watkins DI, Burton DR. 2009. Broadly neutralizing human anti-HIV antibody 2G12 is effective in protection against mucosal SHIV challenge even at low serum neutralizing titers. PLoS Pathog 5:e1000433. https://doi.org/10.1371/journal.ppat.1000433.
37. Mascola JR, Stiegler G, VanCott TC, Katinger H, Carpenter CB, Hanson CE, Beary H, Hayes D, Frankel SS, Birx DL, Lewis MG. 2000. Protection of macaques against vaginal transmission of a pathogenic HIV-1/SIV chimeric virus by passive infusion of neutralizing antibodies. Nat Med 6:207–210. https://doi.org/10.1038/72318.
38. Barouch DH, Whitney JB, Moldt B, Klein F, Oliveira TY, Liu J, Stephenson KE, Chang HW, Shekhar K, Gupta S, Nkolola JP, Seaman MS, Smith KM, Borducchi EN, Cabral C, Smith JY, Blackmore S, Sanisetty S, Perry JR, Beck M, Lewis MG, Rinaldi W, Chakraborty AK, Poignard P, Nussenzweig MC, Burton DR. 2013. Therapeutic efficacy of potent neutralizing HIV-1-specific monoclonal antibodies in SHIV-infected rhesus monkeys. Nature 503:224–228.
39. Klein F, Halper-Stromberg A, Horwitz JA, Gruell H, Scheid JF, Bournazos S, Mouquet H, Spatz LA, Diskin R, Abadir A, Zang T, Dorner M, Billerbeck E, Labitt RN, Gaebler C, Marcovecchio PM, Incesu RB, Eisenreich TR, Bieniasz PD, Seaman MS, Bjorkman PJ, Ravetch JV, Ploss A, Nussenzweig MC. 2012. HIV therapy by a combination of broadly neutralizing antibodies in humanized mice. Nature 492:118–122. https://doi.org/10.1038/nature11604.
40. Horwitz JA, Halper-Stromberg A, Mouquet H, Gitlin AD, Tretiakova A, Eisenreich TR, Malbec M, Gravemann S, Billerbeck E, Dorner M, Buning H, Schwartz O, Knops E, Kaiser R, Seaman MS, Wilson JM, Rice CM, Ploss A, Bjorkman PJ, Klein F, Nussenzweig MC. 2013. HIV-1 suppression and durable control by combining single broadly neutralizing antibodies and antiretroviral drugs in humanized mice. Proc Natl Acad Sci U S A 110:16538–16543. https://doi.org/10.1073/pnas.1315295110.
41. Pietzsch J, Gruell H, Bournazos S, Donovan BM, Klein F, Diskin R, Seaman MS, Bjorkman PJ, Ravetch JV, Ploss A, Nussenzweig MC. 2012. A mouse model for HIV-1 entry. Proc Natl Acad Sci U S A 109:15859–15864. https://doi.org/10.1073/pnas.1213409109.
42. Seaman MS, Janes H, Hawkins N, Grandpre LE, Devoy C, Giri A, Coffey RT, Harris L, Wood B, Daniels MG, Bhattacharya T, Lapedes A, Polonis VR, McCutchan FE, Gilbert PB, Self SG, Korber BT, Montefiori DC, Mascola JR. 2010. Tiered categorization of a diverse panel of HIV-1 Env pseudoviruses for assessment of neutralizing antibodies. J Virol 84:1439–1452. https://doi.org/10.1128/JVI.02108-09.
43. Jiang J, Aiken C. 2007. Maturation-dependent human immunodeficiency virus type 1 particle fusion requires a carboxyl-terminal region of the gp41 cytoplasmic tail. J Virol 81:9999–10008. https://doi.org/10.1128/JVI.00592-07.
44. Joyner AS, Willis JR, Crowe JE, Jr, Aiken C. 2011. Maturation-induced cloaking of neutralization epitopes on HIV-1 particles. PLoS Pathog 7:e1002234. https://doi.org/10.1371/journal.ppat.1002234.
45. Wyma DJ, Jiang J, Shi J, Zhou J, Lineberger JE, Miller MD, Aiken C. 2004. Coupling of human immunodeficiency virus type 1 fusion to virion maturation: a novel role of the gp41 cytoplasmic tail. J Virol 78:3429–3435. https://doi.org/10.1128/JVI.78.7.3429-3435.2004.
46. Wyss S, Dimitrov AS, Baribaud F, Edwards TG, Blumenthal R, Hoxie JA. 2005. Regulation of human immunodeficiency virus type 1 envelope glycoprotein fusion by a membrane-interactive domain in the gp41 cytoplasmic tail. J Virol 79:12231–12241. https://doi.org/10.1128/JVI.79.19.12231-12241.2005.
47. Chen J, Kovacs JM, Peng H, Rits-Volloch S, Lu J, Park D, Zablowsky E, Seaman MS, Chen B. 2015. Effect of the cytoplasmic domain on antigenic characteristics of HIV-1 envelope glycoprotein. Science 349:191–195.
48. Durham ND, Chen BK. 2015. HIV-1 cell-free and cell-to-cell infections are differentially regulated by distinct determinants in the Env gp41 cytoplasmic tail. J Virol 89:9324–9337. https://doi.org/10.1128/JVI.00655-15.
49. Holford NH, Sheiner LB. 1981. Understanding the dose-effect relationship: clinical application of pharmacokinetic-pharmacodynamic models. Clin Pharmacokinet 6:429–453. https://doi.org/10.2165/00003088-198106060-00002.
50. McCoy LE, Falkowska E, Doores KJ, Le K, Sok D, van Gils MJ, Euler Z, Burger JA, Seaman MS, Sanders RW, Schuitemaker H, Poignard P, Wrin T, Burton DR. 2015. Incomplete neutralization and deviation from sigmoidal neutralization curves for HIV broadly neutralizing monoclonal antibodies. PLoS Pathog 11:e1005110. https://doi.org/10.1371/journal.ppat.1005110.
51. Paulson JC, Colley KJ. 1989. Glycosyltransferases. Structure, localization, and control of cell type-specific glycosylation. J Biol Chem 264:17615–17618.
52. Rowell JF, Stanhope PE, Siliciano RF. 1995. Endocytosis of endogenously synthesized HIV-1 envelope protein. Mechanism and role in processing for association with class II MHC. J Immunol 155:473–488.
53. Boge M, Wyss S, Bonifacino JS, Thali M. 1998. A membrane-proximal tyrosine-based signal mediates internalization of the HIV-1 envelope glycoprotein via interaction with the AP-2 clathrin adaptor. J Biol Chem 273:15773–15778. https://doi.org/10.1074/jbc.273.25.15773.
54. Berlioz-Torrent C, Shacklett BL, Erdtmann L, Delamarre L, Bouchaert I, Sonigo P, Dokhelar MC, Benarous R. 1999. Interactions of the cytoplasmic domains of human and simian retroviral transmembrane proteins with components of the clathrin adaptor complexes modulate intracel-

lular and cell surface expression of envelope glycoproteins. J Virol 73:1350–1361.
55. McCoy LE, Groppelli E, Blanchetot C, de Haard H, Verrips T, Rutten L, Weiss RA, Jolly C. 2014. Neutralisation of HIV-1 cell-cell spread by human and llama antibodies. Retrovirology 11:83. https://doi.org/10.1186/s12977-014-0083-y.
56. Zhang H, Zhou Y, Alcock C, Kiefer T, Monie D, Siliciano J, Li Q, Pham P, Cofrancesco J, Persaud D, Siliciano RF. 2004. Novel single-cell-level phenotypic assay for residual drug susceptibility and reduced replication capacity of drug-resistant human immunodeficiency virus type 1. J Virol 78:1718–1729. https://doi.org/10.1128/JVI.78.4.1718-1729.2004.
57. Durham ND, Chen BK. 2016. Measuring T cell-to-T cell HIV-1 transfer, viral fusion, and infection using flow cytometry. Methods Mol Biol 1354:21–38. https://doi.org/10.1007/978-1-4939-3046-3_2.
58. Munro JB, Gorman J, Ma X, Zhou Z, Arthos J, Burton DR, Koff WC, Courter JR, Smith AB, III, Kwong PD, Blanchard SC, Mothes W. 2014. Conformational dynamics of single HIV-1 envelope trimers on the surface of native virions. Science 346:759–763. https://doi.org/10.1126/science.1254426.
59. McCaffrey RA, Saunders C, Hensel M, Stamatatos L. 2004. N-linked glycosylation of the V3 loop and the immunologically silent face of gp120 protects human immunodeficiency virus type 1 SF162 from neutralization by anti-gp120 and anti-gp41 antibodies. J Virol 78:3279–3295. https://doi.org/10.1128/JVI.78.7.3279-3295.2004.
60. Li Y, Rey-Cuille MA, Hu SL. 2001. N-linked glycosylation in the V3 region of HIV type 1 surface antigen modulates coreceptor usage in viral infection. AIDS Res Hum Retroviruses 17:1473–1479. https://doi.org/10.1089/08892220152644179.
61. Edwards TG, Wyss S, Reeves JD, Zolla-Pazner S, Hoxie JA, Doms RW, Baribaud F. 2002. Truncation of the cytoplasmic domain induces exposure of conserved regions in the ectodomain of human immunodeficiency virus type 1 envelope protein. J Virol 76:2683–2691. https://doi.org/10.1128/JVI.76.6.2683-2691.2002.
62. Kalia V, Sarkar S, Gupta P, Montelaro RC. 2005. Antibody neutralization escape mediated by point mutations in the intracytoplasmic tail of human immunodeficiency virus type 1 gp41. J Virol 79:2097–2107. https://doi.org/10.1128/JVI.79.4.2097-2107.2005.
63. Deschambeault J, Lalonde JP, Cervantes-Acosta G, Lodge R, Cohen EA, Lemay G. 1999. Polarized human immunodeficiency virus budding in lymphocytes involves a tyrosine-based signal and favors cell-to-cell viral transmission. J Virol 73:5010–5017.
64. Qi M, Williams JA, Chu H, Chen X, Wang JJ, Ding L, Akhirome E, Wen X, Lapierre LA, Goldenring JR, Spearman P. 2013. Rab11-FIP1C and Rab14 direct plasma membrane sorting and particle incorporation of the HIV-1 envelope glycoprotein complex. PLoS Pathog 9:e1003278. https://doi.org/10.1371/journal.ppat.1003278.
65. Sauter MM, Pelchen-Matthews A, Bron R, Marsh M, LaBranche CC, Vance PJ, Romano J, Haggarty BS, Hart TK, Lee WM, Hoxie JA. 1996. An internalization signal in the simian immunodeficiency virus transmembrane protein cytoplasmic domain modulates expression of envelope glycoproteins on the cell surface. J Cell Biol 132:795–811. https://doi.org/10.1083/jcb.132.5.795.
66. Ohno H, Aguilar RC, Fournier MC, Hennecke S, Cosson P, Bonifacino JS. 1997. Interaction of endocytic signals from the HIV-1 envelope glycoprotein complex with members of the adaptor medium chain family. Virology 238:305–315. https://doi.org/10.1006/viro.1997.8839.
67. Dev J, Park D, Fu Q, Chen J, Ha HJ, Ghantous F, Herrmann T, Chang W, Liu Z, Frey G, Seaman MS, Chen B, Chou JJ. 23 June 2016. Structural basis for membrane anchoring of HIV-1 envelope spike. Science https://doi.org/10.1126/science.aaf7066.
68. Adachi A, Gendelman HE, Koenig S, Folks T, Willey R, Rabson A, Martin MA. 1986. Production of acquired immunodeficiency syndrome-associated retrovirus in human and nonhuman cells transfected with an infectious molecular clone. J Virol 59:284–291.
69. Cohen GB, Gandhi RT, Davis DM, Mandelboim O, Chen BK, Strominger JL, Baltimore D. 1999. The selective downregulation of class I major histocompatibility complex proteins by HIV-1 protects HIV-infected cells from NK cells. Immunity 10:661–671. https://doi.org/10.1016/S1074-7613(00)80065-5.